Mechanism of Induced Circular Dichroism of Amino Acid Ester-Porphyrin Supramolecular Systems. Implications to the Origin of the Circular Dichroism of Hemoprotein

Tadashi Mizutani,* Tadashi Ema, Takashi Yoshida, Thomas Renné, and Hisanobu Ogoshi*

Department of Synthetic Chemistry and Biological Chemistry, Faculty of Engineering, Kyoto University, Yoshida, Sakyo-ku, Kyoto, 606 Japan

*Received February 23, 1994**

Circular dichroism (CD) spectra of the complexes between metalloporphyrins and chiral amino acid derivatives exhibited either split type induced CD or single peak induced CD in the Soret region depending on the host-guest combination. Systematic studies on the complexation of amino acid derivatives by porphyrin hosts indicate that intermolecular hydrogen bonding to the carbonyl group of the guest is necessary for the split type induced CD to occur. Molecular orbital calculations of the rotational strength of a porphyrin-amino acid ester complex by the MNDO method predict that the ICD of porphyrin-amino acid ester complexes is determined by the relative geometry of the carbonyl group and the porphyrin plane. The relative geometry of the chromophores expected from the X-ray crystallographic analysis of a complex between leucine methyl ester and a similar host then gives split type induced CD, in agreement with experiment. These experimental and theoretical results indicate that the coupling between the magnetic transition dipole moment (m_j) and the electric transition dipole moment (μ_j) of a carbonyl group and the electric transition dipole moment (μ_i) of the porphyrin Soret band makes an important contribution to the observed induced CD.

Circular dichroism (CD) has been utilized to investigate chiral properties of compounds. It is specific to a particular chromophore and sensitive to the changes in the relative geometry of the chromophores. It is widely used in protein chemistry to retrieve information on the secondary structure of the peptide backbone and the relative geometry between the prosthetic group and the proteins, which reflects the tertiary structure.[1] In particular, the circular dichroism of the porphyrin chromophore in hemoproteins has drawn the interest of numerous researchers. Both myoglobin and hemoglobin exhibit characteristic induced CD (ICD), and the ICD is frequently used as an important probe for the local structure around heme. Naturally occurring hemoproteins exhibit mostly single peak ICD, and some exhibit split type ICD in the Soret region.[2] Investigation of the origin of the ICD gives useful information on the relative geometry of chromophores around the heme. Woody et al.[3] reported that the aromatic moieties of the amino acid side chains make important contributions to the induced CD observed for myoglobin and hemoglobin based on the molecular orbital calculations. These hemoproteins are structurally complex, and many interactions contribute to the induced CD. Therefore simplified model studies should be helpful in elucidating the mechanism of the ICD in hemoproteins.

We have recently reported molecular recognition studies on amino acid ester-zinc porphyrin systems.[4] Most of the complexes between [*trans*-5,15-bis(2-hydroxy-1-naphthyl)-2,3,7,8,12,13,17,18-octaethylporphyrinato]zinc (**1**) and amino acid esters exhibited split type ICD in the Soret region. We suggested that the induced CD is caused by the coupling between transition moments of the carbonyl group and the porphyrin. In the present paper, we summarize the previously reported ICD data[4] and newly observed ICD data for some porphyrin-guest complexes. Next, we report that molecular orbital calculations on the rotational strength of porphyrin-amino acid ester systems predict the split type ICD. Finally, we comment on the implications of this model study to the origin of optical activity of the hemoprotein.

Experimental Section

^{1}H NMR spectra were recorded on either a Varian Gemini-200, a JEOL GX-400 or a JEOL A-500 FT NMR spectrometer, and chemical shifts are reported relative to internal Me_4Si. UV-vis spectra were recorded on either a Hitachi U-3410 spectrometer or a Hewlett-Packard 8452 diode array spectrophotometer with a thermostated cell compartment. Circular dichroism spectra were recorded on a JASCO J-600 spectropolarimeter with a thermostated cell compartment. The rotational strengths were calculated by fitting the circular dichroism spectra of 350-500-nm region to Gaussian functions: $\Delta\epsilon_1 \exp(-((\lambda - \lambda_1)/\Delta\lambda_1)^2) - \Delta\epsilon_2 \exp(-((\lambda - \lambda_2)/\Delta\lambda_2)^2)$ or $\Delta\epsilon_1 \exp(-((\lambda - \lambda_1)/\Delta\lambda_1)^2)$ where $\Delta\epsilon_1$, $\Delta\epsilon_2$, λ_1, λ_2, $\Delta\lambda_1$ and $\Delta\lambda_2$ are parameters to be determined. The rotational strength (R_1 and R_2) was calculated from these parameters according to $R_i = 2.296 \times 10^{-39} \pi^{1/2} \Delta\epsilon_i \Delta\lambda_i/\lambda_i$, where $i = 1$ or 2.[5] The curve fitting was carried out by the use of Igor, WaveMetrics, Inc. Mass spectra were obtained with a JEOL JMS DX-300 mass spectrometer. Thin layer chromatography (TLC) was performed on Merck Kieselgel 60 F254.

L-Leucine *tert*-butyl ester (Leu-OBu^t), O^1,O^5-dimethyl glutamate (Glu-OMe) and O^1,O^4-dimethyl aspartate (Asp-OMe) were purchased from Sigma. (*S*)-(+)-2-Phenylglycine methyl ester (PhGly-OMe) and N^2-(*tert*-butoxycarbonyl)-L-histidine methyl ester (BOC-His-OMe) were purchased from Kokusan Chemical Works.

[*trans*-5,15-Bis(2-hydroxy-1-naphthyl)-2,3,7,8,12,13,17,18-octaethylporphyrinato]zinc(II) (**1**) and [*trans*-5,15-bis(2-methoxy-1-naphthyl)-2,3,7,8,12,13,17,18-octaethylporphyrinato]zinc(II) (**2**) were prepared according to the published method.[4] Chloro[*trans*-5,15-bis(2-hydroxy-1-naphthyl)-2,3,7,8,12,13,17,18-octaethylporphyrinato]rhodium(III) (**4**) was prepared similarly.[6a] {*trans*-5,15-Bis(2-hydroxy-1-naphthyl)-3,7,13,17-tetramethyl-2,8,12,18-[tetrakis(2-methoxycarbonylethyl)]porphyrinato}zinc(II) (**3**) was prepared by the dipyrromethane method.[6c] {*trans*-5,15-Bis(2-hydroxyphenyl)-10-[2,6-bis(methoxycarbonylmethyl)-phenyl]-2,3,17,18-tetraethylporphyrinato}zinc(II) (**5**) was prepared by coupling of two dipyrromethanes.[7]

* Abstract published in *Advance ACS Abstracts*, July 1, 1994.

(1) Woody, R. W.; Tinoco, I. *J. Chem. Phys.* **1967**, *46*, 4927.
(2) (a) Myer Y. P.; Pande, A. In *The Porphyrins*; Dolphin, D., Ed.; Academic Press: New York, 1978; Vol. 3, pp 271-322. (b) Philipson, K. D.; Tsai, S. C.; Sauer, K. *J. Phys. Chem.* **1971**, *75*, 1440. (c) Houssier, C.; Sauer, K. *J. Am. Chem. Soc.* **1970**, *92*, 779. (d) Gonzalez, M. C.; Weedon, A. C. *Can. J. Chem.* **1985**, *63*, 602.
(3) Hsu, M.-C.; Woody, R. W. *J. Am. Chem. Soc.* **1971**, *93*, 3515.
(4) Mizutani, T.; Ema, T.; Yoshida, T.; Kuroda, Y.; Ogoshi, H. *Inorg. Chem.* **1993**, *32*, 2072.
(5) Harada, N.; Nakanishi, K. *Circular Dichroic Spectroscopy-Exciton Coupling in Organic Stereochemistry*; University Science Books: Mill Valley, CA, 1983.
(6) (a) Aoyama, Y.; Yamagishi, A.; Tanaka, Y.; Toi, H.; Ogoshi, H. *J. Am. Chem. Soc.* **1987**, *109*, 4735. (b) Aoyama, Y.; Uzawa, T.; Saita, K.; Tanaka, Y.; Toi, H.; Ogoshi, H. *Tetrahedron Lett.* **1988**, *29*, 5271. (c) Ogoshi, H.; Sugimoto, H.; Nishiguchi, T.; Watanabe, T.; Matsuda, Y.; Yoshida, Z. *Chem. Lett.* **1978**, 29.

0020-1669/94/1333-3558$04.50/0

Scheme 1

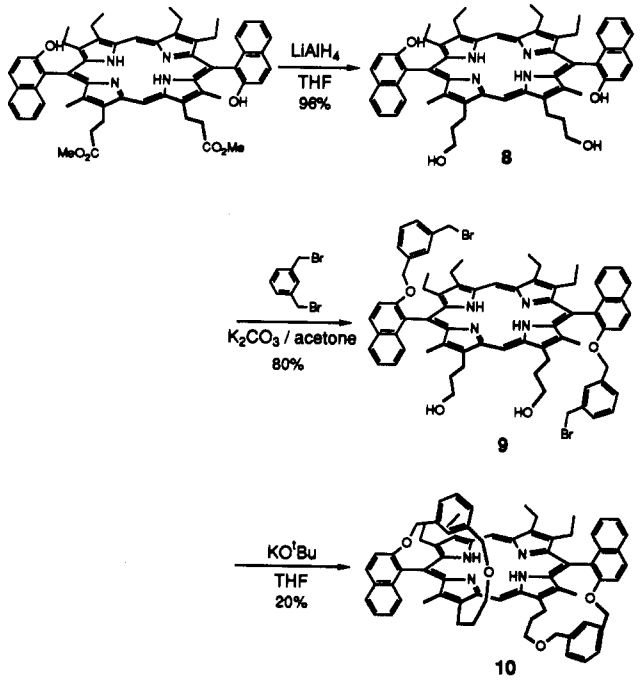

Preparation of *trans*-5,15-Bis(2-hydroxy-1-naphthyl)-8,12-bis(3-hydroxypropyl)-7,13-dimethyl-2,3,17,18-tetraethylporphyrin (8). A solution of *trans*-5,15-bis(2-hydroxy-1-naphthyl)-8,12-bis(2-(methoxycarbonyl)-ethyl)-7,13-dimethyl-2,3,17,18-tetraethylporphyrin[6b] (40 mg, 44 μmol) in dry THF (8 mL) was added dropwise to a suspension of $LiAlH_4$ (30 mg, 790 μmol) in dry THF (2 mL) under N_2. After the suspension was vigorously stirred for 30 min at room temperature in the dark, the reaction was quenched with water and the reaction mixture was extracted with ethyl acetate. The organic layer was dried over Na_2SO_4 and evaporated to dryness to yield **8** (36 mg, 42 μmol, 96%). The product thus obtained was used in the following reaction without further purification: TLC R_f 0.30 ($CHCl_3$:EtOAc = 1:3); ^1H NMR (200 MHz, pyridine-d_5) δ 1.34 (t, 6H, $-CH_2CH_3$), 1.83 (t, 6H, $-CH_2CH_3$), 2.53–2.66 (m, 4H, $-CH_2CH_2CH_2OH$), 2.70 (s, 6H, $-CH_3$), 2.98–3.15, 3.20–3.35 (dq, 4H, $-CH_2CH_3$), 3.88–4.09 (m, 4H, $-CH_2CH_3$), 4.18 (t, 4H, $-CH_2CH_2CH_2OH$), 4.27–4.50 (m, 4H, $-CH_2CH_2CH_2OH$), 7.06 (m, 4H, naphthyl), 7.3–7.5 (m, 2H, naphthyl), 8.03 (d, 2H, naphthyl), 8.23 (d, 2H, naphthyl), 8.48 (d, 2H, naphthyl), 10.41 (s, 1H, meso), 10.85 (s, 1H, meso), –1.62 (br s, 2H, NH); UV–vis ($CHCl_3$) λ_{max} [nm] 412.5, 510, 544, 574.5, 628; FABMS (3-nitrobenzyl alcohol) *m/z* 851 (M + 1).

Preparation of the Precursor of the Bridged Chiral Porphyrin 9. A mixture of the tetrahydroxyporphyrin derivative (**8**) (13 mg, 15.3 μmol), *m*-xylylene dibromide (116 mg, 440 μmol), and K_2CO_3 (20 mg, 145 μmol) in dry acetone (1 mL) was refluxed for 3 h under N_2 with vigorous stirring. After filtration to remove K_2CO_3, the solution was evaporated. The residue was purified by chromatography (silica gel column, $CHCl_3$) to yield **9** (14.9 mg, 12.3 μmol, 80%): TLC R_f 0.50 ($CHCl_3$:EtOAc = 1:1); ^1H NMR (200 MHz, $CDCl_3$) δ 0.80 (t, 6H, $-CH_2CH_3$), 1.8 (t, 6H, $-CH_2CH_3$), 2.1 (s, 6H, $-CH_3$), 2.2–2.4 (m, 4H, $-CH_2CH_2CH_2OH$), 2.5–2.8 (m, 4H, $-CH_2CH_3$), 3.2 (s, 4H, $PhCH_2Br$), 3.8–4.2 (m, 12H, $-CH_2CH_3$, $-CH_2CH_2CH_2OH$), 5.2 (dd, 4H, OCH_2Ph), 10.3 (s, 1H, meso), 10.4 (s, 1H, meso), –2.0 (br s, 2H, NH); IR (KBr) ν_{OH} 3350 cm^{-1}, no C=O peak; UV–vis ($CHCl_3$) λ_{max} [nm] 416.5, 511, 544, 578, 629; FABMS (3-nitrobenzyl alcohol) *m/z* 1215 ($M^+(^{79}Br)$ + 1), 1216, 1217($M^+(^{79}Br^{81}Br)$ + 1), 1218, 1219 ($M^+(^{81}Br)$ + 1).

Preparation of the C_2-Symmetric Chiral Porphyrin 10. The dibromoporphyrin derivative (**9**) (7.5 mg, 6.2 μmol) dissolved in a small amount of dry THF was quickly added to a dry THF solution (700 mL) containing KO^{t}Bu (100 mg, 893 μmol). The highly diluted solution (9 μM) was refluxed under Ar for 3 h. After the reaction was quenched with a small amount of water, the solvent was removed by rotary evaporation. The resultant product mixture was dissolved in $CHCl_3$ and passed through a short pad of Cerite to remove byproducts. The crude product was purified by preparative TLC using $CHCl_3$–EtOAc (20:1) as the eluent (an average yield was 20%). Recrystallization from CH_2Cl_2–MeOH gave purple needles: TLC R_f 0.4 ($CHCl_3$:EtOAc = 20:1); ^1H NMR (400 MHz, $CDCl_3$) δ 0.97 (t, 6H, $-CH_2CH_3$, *J* = 7.4 Hz), 1.82 (t, 6H, $-CH_2CH_3$, *J* = 7.6 Hz), 2.11 (s, 6H, $-CH_3$), 2.42 (dq, 2H, $-CH_2CH_3$), 2.7–2.9 (m, 4H, $-CH_2CH_2CH_2-$), 2.89 (dq, 2H, $-CH_2CH_3$), 3.5–3.65 (dq, 4H, $-CH_2CH_2CH_2O-$), 3.6–3.75 (m, 2H, $-CH_2CH_2CH_2O-$), 3.8–4.1 (m, 4H, $-CH_2CH_3$), 4.08 (d, 2H, $-OCH_2Ph$, *J* = 13.7 Hz), 4.35–4.43 (m, 2H, $-CH_2CH_2CH_2O-$), 4.56 (d, 2H, OCH_2Ph, *J* = 13.9 Hz), 4.79 (d, 2H, naphthyl–OCH_2Ph, *J* = 12.7 Hz), 5.28 (d, 2H, naphthyl–OCH_2Ph, *J* = 12.7 Hz), 6.81 (m, 4H, naphthyl, phenyl), 6.93 (t, 2H, naphthyl, *J* = 8.4 Hz), 7.01 (d, 4H, phenyl, *J* = 4.8 Hz), 7.07 (s, 2H, phenyl), 7.31 (t, 2H, naphthyl, *J* = 8.0 Hz), 7.66 (d, 2H, naphthyl, *J* = 9.2 Hz), 8.00 (d, 2H, naphthyl, *J* = 8.2 Hz), 8.25 (d, 2H, naphthyl, *J* = 9.2 Hz), 10.10 (s, 1H, meso), 10.23 (s, 1H, meso), –1.91 (br s, 2H, NH); UV–vis ($CHCl_3$) λ_{max} [nm (log ε)] 416.5 (5.40), 510.5 (4.28), 545 (3.78), 577 (3.90), 629 (3.30); HRMS (FAB, 3-nitrobenzyl alcohol) found, 1055.5470, calcd 1055.5480. The racemic mixture of **10** was resolved by means of HPLC (CHIRALCEL OD, Daicel, hexane–2-propanol = 8:2). The first fraction was used for the CD measurement.

Preparation of 5-(2,6-Dimethoxyphenyl)-10,15,20-triphenylporphyrin (13). A mixture of pyrrole (1.125 g, 16.8 mmol), benzaldehyde (1.35 g, 12.7 mmol) and 2,6-dimethoxybenzaldehyde (0.7 g, 4.21 mmol) was added to refluxed propionic acid (60 mL), and the resulting dark reaction mixture was stirred under reflux for 1 h. After the reaction mixture was cooled, the solvent was distilled off under reduced pressure. The remaining black residue was chromatographed on a silica gel column (φ = 3 × 15 cm, $CHCl_3$:hexane = 8:2) to give a mixture of tetraphenylporphyrin (TPP, the first fraction) and the desired compound (the second fraction). Further purification by chromatography on a silica gel column (φ = 1.5 × 32 cm, $CHCl_3$:hexane = 4:3) afforded **13** (283 mg). Recrystallization from $CHCl_3$–MeOH gave purple crystals (147 mg): mp > 300 °C; TLC R_f = 0.17 ($CHCl_3$:hexane = 3:1); ^1H NMR ($CDCl_3$, 500 MHz) 3.51(s, 6H, OCH_3), 7.00 (d, 2H, phenyl), 7.71–7.74 (m, 10H, phenyl), 8.18–8.20 (m, 6H, phenyl), 8.77–8.79 (m, 8H, β-H), –2.71 (br s, 2H, NH); UV–vis ($CHCl_3$) λ_{max} [nm (log ε)] 419 (5.63), 515 (4.26), 549 (3.84), 589 (3.74), 649 (3.65); FAB MS (3-nitrobenzyl alcohol) *m/z* 675 (MH^+).

Preparation of 5-(2,6-Dihydroxyphenyl)-10,15,20-triphenylporphyrin (11). To a solution of **13** (50 mg, 74 μmol) in dry CH_2Cl_2 (3 mL) was added 0.7 mL of 1 M BBr_3 in CH_2Cl_2 at –40 °C, and the solution was allowed to warm to room temperature slowly. After the reaction mixture was stirred at room temperature for 5.5 h, the solution was cooled to –30 °C and MeOH (1 mL) was added carefully. The reaction mixture was poured into aqueous $NaHCO_3$, washed with H_2O, and then dried over Na_2SO_4. Separation by preparative TLC eluted with $CHCl_3$ gave the target porphyrin (45 mg, 70%). Recrystallization from $CHCl_3$–MeOH gave purple crystals: mp > 300 °C; TLC R_f = 0.25 ($CHCl_3$); ^1H NMR ($CDCl_3$, 500 MHz) δ 4.69 (br s, 2H, OH), 6.98 (d, 2H, phenyl 3-H), 7.60 (t, 1H, phenyl 4-H), 7.73–7.78 (m, 9H, phenyl), 8.18–8.19 (m, 6H, phenyl), 8.85–8.91 (m, 8H, β-H), –2.74 (br s, 2H, NH); IR (KBr) 3529 cm^{-1} (OH); UV–vis λ_{max} [nm (log ε)] 418 (5.65), 549 (3.76), 646 (3.46), 515 (4.29), 588 (3.72); HRMS (FAB, 3-nitrobenzyl alcohol) calcd for $C_{44}H_{30}O_2N_4$ (M^+) 646.2368, found 646.2378.

Zinc was inserted according to the literature method.[8] The zinc complex was purified by preparative TLC ($CHCl_3$:EtOAc = 20:1) and recrystallized from $CHCl_3$–hexane: TLC R_f = 0.25 ($CHCl_3$:hexane = 20:1); ^1H NMR ($CDCl_3$, 500 MHz) δ 4.73 (br s, 2H, OH), 6.94 (d, 2H, phenyl), 7.58 (t, 1H, phenyl), 7.72–7.79 (m, 9H, phenyl) 8.18–8.21 (m, 6H, phenyl), 8.93–9.00 (m, 8H, β-H); UV–vis ($CHCl_3$) λ_{max} [nm (log ε)] 423 (5.63), 553 (4.22), 595 (3.56).

Results and Discussion

Induced CD of the Amino Acid Ester–Porphyrin Systems. The CD spectra in the Soret region of metalloporphyrins (**1–7**) induced by complexation with chiral amino acid derivatives (Ala–OMe,

(7) Mizutani, T.; Ema, T.; Tomita, T.; Kuroda, Y.; Ogoshi, H. *J. Am. Chem. Soc.* **1994**, *116*, 4240.

(8) Smith, K. M. *Porphyrins and Metalloporphyrins*; Elsevier; Amsterdam, 1975; pp 884–885.

(9) (a) Moscowitz, A.; Mislow, K.; Glass, M. A. W.; Djerassi, C. *J. Am. Chem. Soc.* **1962**, *84*, 1945. (b) Moscowitz, A.; Hansen, A. E.; Forster, L. S.; Rosenheck, K. *Biopolym. Symp.* **1964**, *1*, 75. (c) Snatzke, G. *Optical Rotatory Dispersion and Circular Dichroism in Organic Chemistry*; Heyden and Son Ltd.: London, 1967.

(10) (a) Labhart, H.; Wagniere, G. *Helv. Chim. Acta* **1959**, *42*, 2219. (b) Schippers, P. H.; Dekkers, H. P. J. M. *J. Am. Chem. Soc.* **1983**, *105*, 79.

(11) Tinoco, I. *Adv. Chem. Phys.* **1962**, *4*, 113.

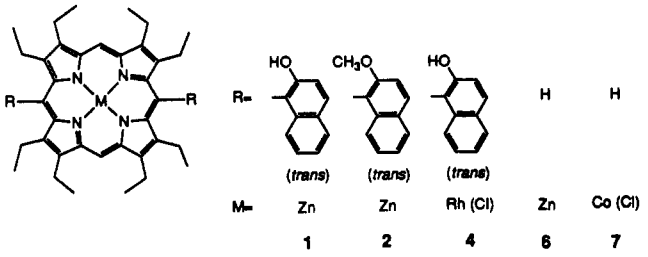

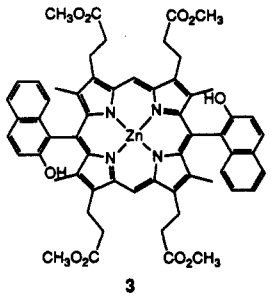

3

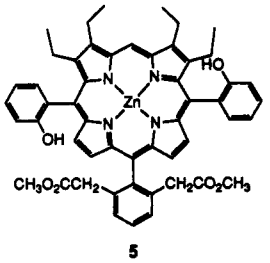

5

Val–OMe, Leu–OMe, Pro–OMe, Glu–OMe, Asp–OMe, Phe–OMe, Trp–OMe, Met–OMe, PhGly–OMe, BOC–His–OMe, Leu–OBu^t, and leucinol) were measured in $CHCl_3$ under the conditions that more than 90% of the porphyrin is complexed with the amino acid derivatives. The binding capabilities of these hosts **1**–**7** are briefly summarized first. Host **1** acts as a two-point recognition host by using two recognition sites, a coordination site (the Zn ion) and a hydrogen-bonding site (the OH group).[4] The amino acid esters were bound to host **1** via (1) coordination interaction between the amino group of the guest and the zinc ion of the host and (2) the hydrogen-bonding interaction between the carbonyl group of the guest and the hydroxyl group of the host (Figure 1). Host **2** is a reference host, having only a coordination site (the Zn ion). Host **2** acts as a one-point recognition host. Hosts **3**–**5** have binding capabilities similar to those of host **1**. In host **3** additional ester groups were introduced on the pyrrole β position. In host **4**, zinc was replaced with rhodium. The coordination interaction is stronger in rhodium porphyrin than zinc porphyrin, but the configuration in the host–guest complex is essentially the same as host **1**. In host **5**, phenyl groups were introduced at the meso position. Hosts **6** and **7** are the Zn and Co complexes of octaethylporphyrin (OEP), respectively. These hosts **6** and **7** have only a coordination site and act as a one-point fixation host. In chiral porphyrin **10**, aromatic

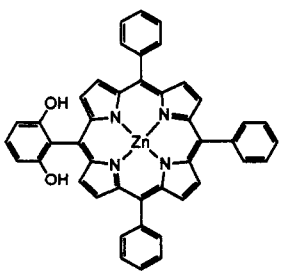

11

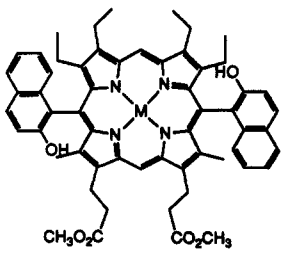

12: M = Rh(Cl)

chromophores are fixed by covalent bonds, and it is a good model to investigate the effect of a covalently fixed aromatic group on the induced CD.

Porphyrin host **1** exhibited split type ICD in the Soret region upon binding almost all the amino acid esters examined (Ala–OMe, Val–OMe, Leu–OMe, Pro–OMe, Phe–OMe, Trp–OMe, PhGly–OMe, Glu–OMe, Asp–OMe, Met–OMe, Leu–OBu^t)

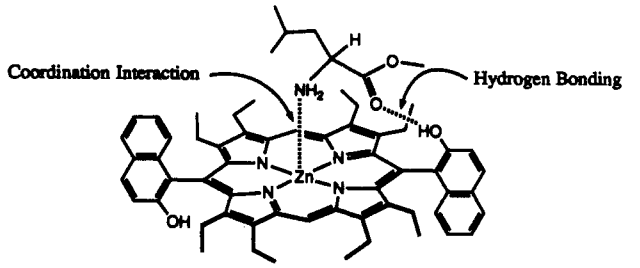

Figure 1. Schematic representation of two-point adduct of host **1** and Leu–OMe. Coordination interaction and hydrogen bonding are shown in dotted lines.

Table 1. Rotational Strength of Amino Acid Ester–**1** (**2**–**6**) Complexes[a]

guest	host	λ_1, nm	$\Delta\epsilon_1$, M^{-1}. cm^{-1}	R_1/ 10^{-40}, cgs	λ_2, nm	$\Delta\epsilon_2$, M^{-1}. cm^{-1}	R_2/ 10^{-40}, cgs	ref
Leu–OMe	1	422.2	53.3	32.3	427.2	−49.0	−36.5	4
Val–OMe	1	424.5	38.9	31.5	430.2	−50.8	−30.2	4
Ala–OMe	1	424.5	22.8	19.2	429.3	−24.0	−18.0	4
Phe–OMe	1	422.6	37.1	19.0	429.3	−50.2	−29.9	4
Trp–OMe	1	423.0	64.6	38.3	429.1	−64.3	−51.4	4
PhGly–OMe	1	422.3	17.9	17.0	427.6	−21.4	−26.3	this work
Leu–OBu^t	1	425.0	38.5	30.7	430.3	−51.0	−36.3	4
Glu–OMe	1	422.9	16.6	16.1	429.9	−19.9	−12.5	4
Asp–OMe	1	424.0	24.3	20.6	429.6	−30.8	−20.3	4
Met–OMe	1	422.1	10.4	10.9	428.1	−10.1	−13.4	this work
Pro–OMe	1	422.3	13.6	17.6	428.1	−8.9	−14.2	this work
leucinol	1	*b*	*b*	*b*	431.0	−5.0	−3.6	4
BOC–His–OMe	1	*c*	*c*	*c*	*c*	*c*	*c*	this work
Phe–OMe	2	425.0	−14.2	−3.8	*b*	*b*	*b*	4
Trp–OMe	2	426.0	−7.0	−1.7	*b*	*b*	*b*	4
PhGly–OMe	2	422.1	−4.7	−5.7	*b*	*b*	*b*	this work
leucinol	2	*b*	*b*	*b*	431.4	−9.6	−3.1	4
Leu–OMe	3	420.0	9.2	11.0	425.6	−12.0	−19.0	this work
Leu–OMe	4	411.2	14.6	29.8	427.2	−8.2	−24.1	this work
Leu–OMe	5	*b*	*b*	*b*	430.2	−2.1	−1.3	this work
Phe–OMe	6	411.1	−5.0	−7.5	*b*	*b*	*b*	this work

[a] At 15 °C in $CHCl_3$, the concentrations of hosts were 4.8×10^{-6} to 5.3×10^{-6} M, and the guest concentration was adjusted so that 90–98% of the host was complexed with guest. The values of $\Delta\epsilon_1$, $\Delta\epsilon_2$, R_1, and R_2 were corrected for the percentage of complexation. All guests were L-(*S*-) configuration. [b] Not observed. [c] No peak observed between 350 and 500 nm.

(Figure 2, a–d). Only the complex between host **1** and BOC–His–OMe did not exhibit split type ICD. This may be ascribed to the different binding mode of the complex (*vide infra*). In the case of the split type ICD, the rotational strength R_a was calculated on the assumption that the ICD is composed of two Gaussian curves with opposite signs, and λ_{max} (λ_1, λ_2), $\Delta\epsilon_{max}$ ($\Delta\epsilon_1$, $\Delta\epsilon_2$), and R_a (R_1, R_2) are calculated and listed in Table 1. The following observations indicate that the split type ICD are caused by the hydrogen bonding interaction between host **1** and amino acid esters: (1) In contrast to the generally observed split type ICD for host **1**, the reference host **2**, which is the methoxy derivative of host **1** and unable to form hydrogen bonding to a guest, showed negligibly small ICD upon complexation with aliphatic amino acid esters such as Leu–OMe, Val–OMe, Ala–OMe, Glu–OMe, Asp–OMe, Met–OMe, Pro–OMe, and Leu–OBu^t ($|\Delta\epsilon| < 6$ for all these guests). (2) For the complexes between **1** and the amino acid derivatives, the correlation between the rotational strength and the hydrogen bonding free energy ($-\Delta\Delta G°_{HB}$) is observed as shown in Figure 3. This correlation suggests that the hydrogen bonding is a driving force of the ICD. A correlation line was drawn by a least-squares method for aliphatic amino acid esters bearing no chromophores on a side chain (Ala–OMe, Val–OMe, and Leu–OMe). The guests bearing chromophores on a side

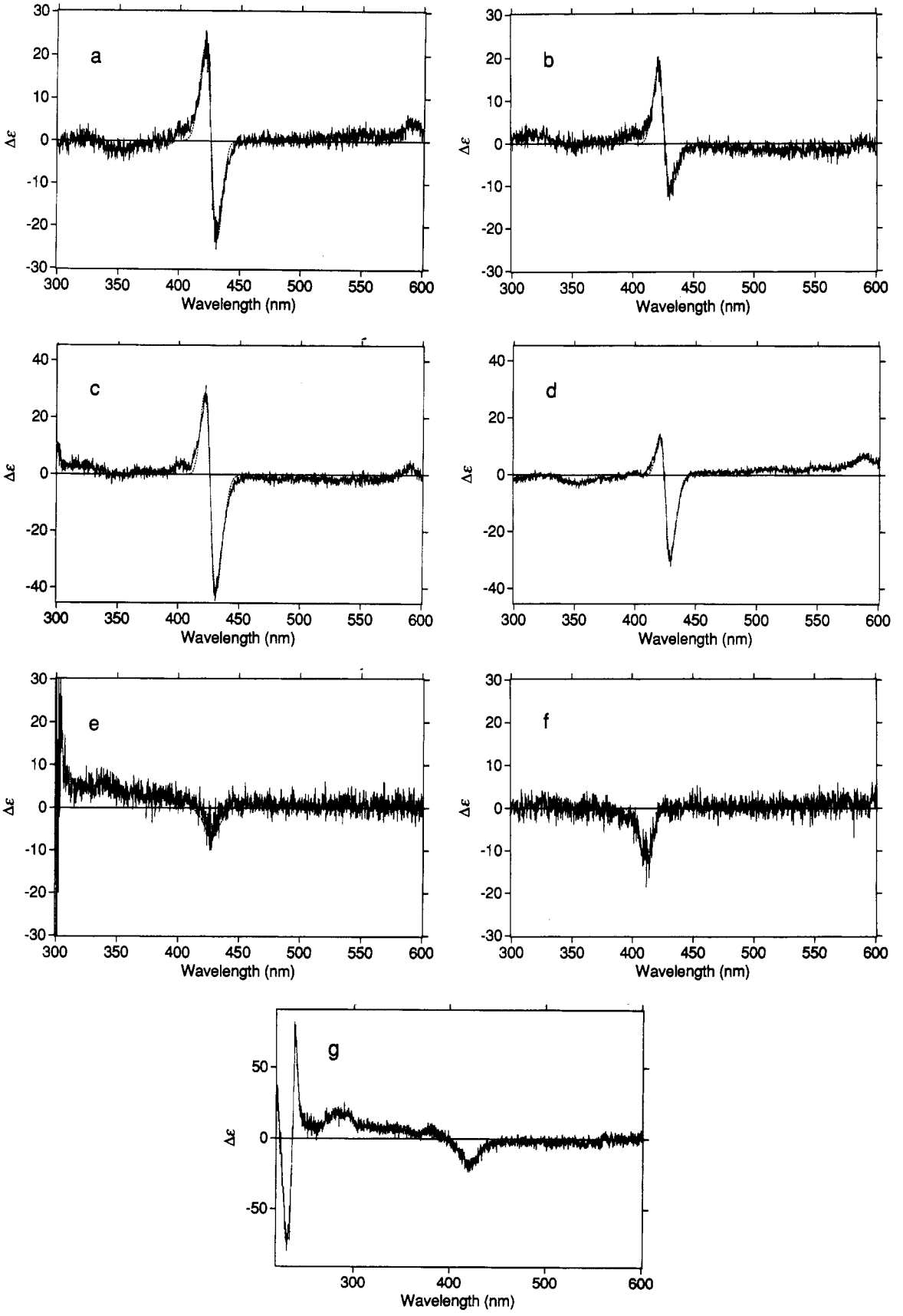

Figure 2. Induced CD of amino acid ester–host **1** (**2**, or **6**) complexes: (a) L-Val–OMe–host **1** complex, (b) L-Pro–OMe–host **1** complex, (c) L-Trp–OMe–host **1** complex, (d) L-PhGly–OMe–host **1** complex, (e) L-Trp–OMe–host **2** complex, (f) L-Phe–OMe–host **6** complex, in $CHCl_3$ at 15°C and (g) **10** in *n*-hexane–ethanol (10/1). Least-squares fit of Gaussian functions are shown in dotted lines. The host and guest concentrations were 4.8×10^{-6} and 3.3×10^{-3} M, respectively.

chain showed deviation from the correlation line (*vide infra*). These observations suggest that the hydrogen bonding between the naphthyl OH group of host **1** and the carbonyl oxygen of the guest affected the conformation of host or guest and thus resulted in the present ICD. It should be noted that the leucinol–**1** complex exhibited very weak ICD in the Soret region, although a hydrogen-

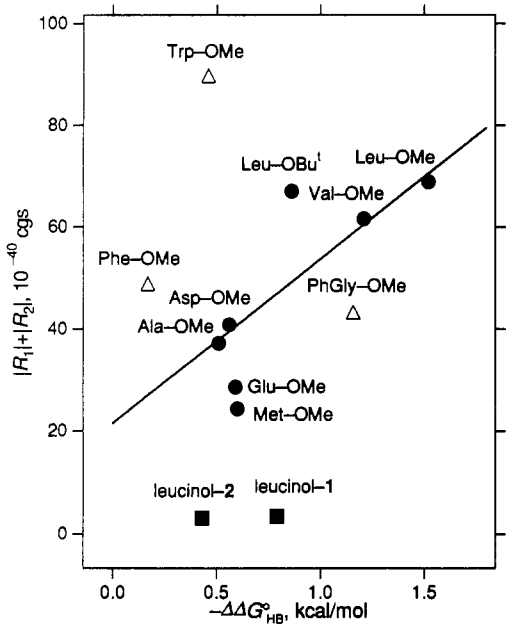

Figure 3. Plot of the rotational strength ($|R_1| + |R_2|$) against hydrogen-bonding energy ($-\Delta\Delta G°_{HB}$). R_1 and R_2 were obtained by a least-squares curve fitting assuming that the spectra consist of two Gaussian peaks. The values of $-\Delta\Delta G°_{HB}$ were calculated from $-\Delta\Delta G°_{HB} = -RT \ln[K_a(\mathbf{1}\text{(or }\mathbf{2})\text{–guest})/K_a(\text{reference host–guest})]$, where the reference host is [5,15-bis(1-naphthyl)-2,3,7,8,12,13,17,18-octaethylporphyrinato]zinc for leucinol–**1**, leucinol–**2** and Leu–OBu^t–host **1** complexation and from $-\Delta\Delta G°_{HB} = -RT \ln[\{K_a(\mathbf{1}\text{–guest})/K_a(\mathbf{2}\text{–guest})\}/\{K_a(\mathbf{1}\text{–reference guest})/K_a(\mathbf{2}\text{–reference guest})\}]$, where the reference guest is 4-heptylamine for other complexation.[4] All values of K_a were determined at 15 °C in a $CHCl_3$ solution by UV–vis spectrophotometric titration. K_a(**1**–PhGly–OMe) = 10 990 ± 110 M^{-1}, K_a(**2**–PhGly–OMe) = 520 ± 10 M^{-1}, K_a(**1**–Met–OMe) = 2460 ± 50 M^{-1}, and K_a(**2**–Met–OMe) = 310 ± 10 M^{-1}. Other values of K_a were reported in ref 4. A line was drawn by a least-squares method to the aliphatic guests (Leu–OMe, Val–OMe, Ala–OMe).

bonding interaction was proved to be operating in the complex.[4] This result, combined with the above evidence for the hydrogen bonding as a driving force, indicates both the presence and the fixation of the carbonyl group play an essential role in the present ICD.

Chromophores of the side chain of the guest also give rise to the ICD. For aromatic amino acid esters (Phe–OMe, Trp–OMe, and PhGly–OMe), Met–OMe, and leucinol, the obvious deviations from the correlation line are observed (Figure 3). The larger magnitude of $|R_1| + |R_2|$ for Phe–OMe and Trp–OMe can be ascribed to the coupling between the electric transition moment of the aromatic side chain and that of the Soret transition of porphyrin. The aromatic amino acid esters each exhibited a small single peak ICD upon complexation with the reference host **2** (Figure 2e). Therefore the ICD of **1** caused by Phe–OMe and Trp–OMe can be understood as the superposition of effects of two perturbers, the carbonyl group and the aromatic group. Other chromophores in the side chains (–$CONH_2$, –COOMe, and –SMe) showed smaller effects on the ICD. These chromophores are extended far from the porphyrin plane and may be fluctuating in the complex. Among the chromophores in the side chain, only aromatic chromophores, especially an indole ring, were found to make important contributions to the ICD.

Unsymmetrical ICD was observed for some of the complexes between host **1** and nonaromatic guests. For example, the complex between Leu–OBu^t and **1** exhibited unsymmetrical ICD (Table 1) compared to the symmetrical ICD of the Leu–OMe–**1** complex. Most complexes showed the ICD pattern that the rotational strengths in the longer wavelength peak (R_2) are larger in magnitude than that in the shorter wavelength peak (R_1) except for Pro–OMe and Glu–OMe. These observations may suggest that Leu–OBu^t, Pro–OMe, and Glu–OMe have a somewhat different conformation in the complexes.

The rotational strengths of complexes between other hosts **3**–**6** and various amino acid esters or an amino alcohol are also listed in Table 1. A similar split type ICD was also observed between Leu–OMe and hosts **3** and **4**. This indicates that the split type ICD is not limited to the zinc porphyrin nor 5,15-diaryloctaethylporphyrin. In contrast, one-point recognition hosts **6** and **7** did not show split type ICD. The complexes between Leu–OMe and **6** (or **7**) showed no ICD in the Soret region. This also supports the previous conclusion that two-point fixation as driven by the coordination interaction and the hydrogen bonding interaction is necessary for the ICD to be observed. Effects of aromatic perturbers are also obvious in the case of one-point recognition hosts. As shown in Figure 2f, the complex between Phe–OMe and **6** exhibited small single peak ICD in the Soret region. This again indicates that the aromatic chromophore induced single peak CD in the Soret band. Finally, as an example of CD caused by a covalently linked chromophore, the CD of compound **10** is shown in Figure 2g. The rotational strength was -47.9×10^{-40} cgs. The parent porphyrin **8** did not exhibit a peak in the Soret region in the CD spectrum. The PM3 calculation[12] of the stable conformation of **10** indicates that the porphyrin plane is flat. Therefore the origin of the CD is not the puckering of porphyrin but the coupling between the benzene chromophore and the porphyrin chromophore. The observed value of the rotational strength gives an estimate of the rotational strength caused by fixed benzene chromophores.

Mechanism of the Induced CD. The split type ICD was observed only for the two-point fixation complexes. The mechanism of the ICD can be classified into the following: (1) conformational change (fixation) of the guest and (2) conformational change (fixation) of the host. If the guest conformational change mechanism is operating, it is clear that the ICD is caused by the –$CH(NH_2)CO$– part of the amino acid ester because the split type ICD was observed for all the amino acid esters with varying side chains (aliphatic and aromatic). In spite of the diversity of the guest structure, all the observed ICD for L-amino acid esters exhibited a positive peak at a shorter wavelength region (423 nm) and a negative peak at a longer wavelength region (429 nm). Therefore the ICD seems to reflect the configuration around the chiral carbon directly.

We considered three possible mechanisms for the induced CD observed for the amino acid ester–porphyrin supramolecular system: (1) binding of the guest molecule by the host through coordination and hydrogen-bonding interactions fixes the relative orientation of the two chromophores (the carbonyl group and the porphyrin group), and the coupling between the magnetic transition moment (the n–π^* transition) and the electric transition moment (the π–π^* transition) of the carbonyl group and the electric transition moment of the porphyrin Soret band causes the ICD; (2) the complexation with amino acid esters causes the tilting of the naphthyl group of the host and the coupling between the electric transition moment of the naphthyl group and that of the porphyrin Soret band induces the observed ICD; (3) puckering of the porphyrin plane caused by the complexation with chiral amino acid esters results in the ICD. The second mechanism was ruled out because this mechanism cannot explain the split type ICD observed in the Soret band.[4] We discuss the possibility of the first mechanism in detail. The third mechanism is also investigated by comparing the degree of puckering of the present system with that of the other well characterized synthetic porphyrins.

Carbonyl–Porphyrin Coupling Mechanism. The coupling between the magnetic transition moment of a carbonyl group and the electric transition moment of ethylene or phenyl groups is considered to be an origin of optical activity of many ketones.[9]

(12) MOPAC Ver. 5 and Ver. 6. Stewart, J. J. P. *QCPE Bull.* **1989**, *9*, 10.

For example, β,γ-unsaturated ketones show a greater increase in intensity of CD than for the corresponding saturated ketones. This enhancement in CD is attributed to the coupling between the magnetic transition moment of the carbonyl group and the electric transition moment of the ethylene group.[10] In the present supramolecular system, the similar coupling between the electric transition moment of the porphyrin Soret band and the magnetic transition moment of the carbonyl n–π^* transition of the guest can cause the induced CD, if the two chromophores are fixed by intermolecular forces.

Several experimental results support this mechanism. All the complexes between amino acid esters (Ala–OMe, Val–OMe, Leu–OMe, Phe–OMe, Trp–OMe, PhGly–OMe, Leu–OBu^t, Pro–OMe, Glu–OMe, Asp–OMe, and Met–OMe) and host **1**, where the hydrogen bonding between the carbonyl group of the guest and the hydroxyl group of the host is operating, exhibited split type ICD. In contrast, the complexes between amino acid esters and host **2**, where no hydrogen bonding is operating, exhibited different ICD patterns in the Soret region: no appreciable ICD for aliphatic guests or small single peak ICD for aromatic guests. These results suggest that the hydrogen bonding is the driving force of the ICD. The fact that the leucinol–host **1** complex exhibited very small ICD and the hydrogen bonding is operating in this leucinol–**1** complex demonstrates that the presence of the carbonyl group is essential for the ICD. Based on these observations, we can assume that the hydrogen bonding to the carbonyl group of the guest will fix the relative geometry of the carbonyl group and the effective coupling between the carbonyl transition moment and the porphyrin transition moment results in the split type ICD. The fact that the variation in the side chains (bulkiness, polarity etc.) did not affect the split pattern of the ICD indicates that the ICD is caused by the interaction between the residual part (–CH(NH_2)CO–) of the amino acid ester and the porphyrin. The intensity of the ICD varied with varying the side chains, suggesting that the magnitude of interaction changes with changing the structure of the side chains. As shown in Figure 3, the rotational strength ($|R_1|+|R_2|$) increases as the hydrogen bonding free energy ($|\Delta\Delta G°_{HB}|$) increases. This correlation implies that a strong hydrogen bond will fix the carbonyl orientation in the host–guest complex, resulting in the increase in ICD intensities. A weak hydrogen bond will allow the carbonyl group to fluctuate to some extent, and it will bring about the averaging of the rotational strength for a range of conformers, thus reducing the intensity of the observed ICD. The fact that the amino acid ester–host **2** complexes did not exhibit any ICD in the Soret region except for Phe–OMe, Trp–OMe, and PhGly–OMe is also consistent with the above mechanism, since no fixation of the carbonyl group can be expected in the amino acid ester–**2** complexes. Therefore, if this mechanism is valid, the mobility of the guest in the complex can be sensitively detected by the ICD measurements.

Calculation of the Rotational Strength Induced in the Soret Band by the Coupling with the Carbonyl Group. Tinoco's formalism was used to calculate the rotational strength induced in the Soret band by the interaction with the carbonyl group.[11] The basic assumption in that theory is that the electrons in the molecule can be assigned to particular groups. This assumption is valid in the present system, because the two chromophores (the carbonyl group and the porphyrin group) are well isolated. Mixing of the wave functions of the carbonyl group to the wave functions associated with the porphyrin Soret transition was assumed to cause the induced CD. Expressions for the rotational strength by this mechanism were obtained by a perturbation approximation.[4, 11] The coupling between the magnetic transition dipole moment (the n–π^* transition) and the electric transition dipole moment (the π–π^* transition) of the carbonyl group and the electric transition dipole moment of the porphyrin chromophore was explicitly considered. The rotational strength was calculated from the following equations.

$$R_a = \frac{2\nu_a \,\mathrm{Im}\left\langle \phi_{i0}\,\phi_{ia}\left|\frac{e^2}{r_{ij}}\right|\phi_{jb}\,\phi_{j0}\right\rangle \vec{\mu}_{i0a}\cdot\vec{m}_{jb0}}{h(\nu_a^2-\nu_b^2)} -$$

$$\frac{2\pi}{c}\,\frac{\nu_a\,\nu_c\left\langle \phi_{i0}\,\phi_{ia}\left|\frac{e^2}{r_{ij}}\right|\phi_{jc}\,\phi_{j0}\right\rangle \vec{R}_{ij}\cdot\vec{\mu}_{i0a}\times\vec{\mu}_{j0c}}{h(\nu_a^2-\nu_c^2)}$$

$$\vec{\mu}_{i0a} = e\langle\phi_{i0}|\vec{r}_i|\phi_{ia}\rangle$$

$$\vec{m}_{jb0} = \frac{eh}{4\pi mci}\langle\phi_{jb}|\vec{r}_j\times\vec{\nabla}_j|\phi_{j0}\rangle$$

where i denotes group i (porphyrin), j denotes group j (carbonyl group), ϕ_{i0} and ϕ_{j0} represent the ground state of the chromophores i and j, respectively, ϕ_{ia} represents the singlet excited state of the porphyrin Soret transition, ϕ_{jb} represents the singlet excited state of the carbonyl n–π^* transition, ϕ_{jc} represents the singlet excited state of the carbonyl π–π^* transition, μ_{i0a} and m_{jb0} are the electric transition dipole moment and the magnetic transition dipole moment, respectively, and r_{ij} is the distance between the electron belonging to group i and the electron belonging to group j. R_{ij} is the position vector of the center of chromophore j relative to the center of chromophore i. ν_a, ν_b, and ν_c are the transition wavenumbers for the Soret transition, the n–π^* transition, and the π–π^* transition of the carbonyl group, respectively, h is Planck's constant, $-e$ is the electron charge, m is the electron mass, c is the velocity of light, and ∇ is the gradient operator. Molecular orbital calculations were carried out by use of the MNDO method for the optimized geometry of porphyrin **1** and glycine methyl ester.[12] For the calculation of the molecular orbitals of **1**, configuration interaction (CI) calculations were carried out according to the Gouterman four-orbital model.[13] The electric transition moment, the magnetic transition moment, and the perturbation matrix element were calculated by expressing the Slater atomic orbital with Gaussian functions.[14] Whitten's

$$\phi_{i0} = \sum_m c_m \exp(-\alpha_m|\vec{r}-\vec{R}_m|^2)$$

$$\phi_{ia} = \sum_n c_n \exp(-\alpha_n|\vec{r}-\vec{R}_n|^2)$$

$$\phi_{j0} = \sum_p c_p \exp(-\alpha_p|\vec{r}-\vec{R}_p|^2)$$

$$\phi_{jb} = \sum_q c_q \exp(-\alpha_q|\vec{r}-\vec{R}_q|^2)$$

$$\phi_{jc} = \sum_r c_r \exp(-\alpha_r|\vec{r}-\vec{R}_r|^2)$$

lobe orbitals were employed to express the Gaussian functions.[15] The matrix element, the electric transition moment and the magnetic transition moment were calculated by the following equations.

(13) (a) Gouterman, M. *J. Mol. Spectrosc.* **1961**, *6*, 138. (b) Gouterman, M.; Wagniere, G. H. *J. Mol. Spectrosc.* **1963**, *11*, 108.
(14) (a) Donkersloot, M. C. A.; Buck, H. M. *J. Mol. Structure (THEOCHEM)* **1986**, *137*, 347. (b) Mizutani, T.; Nakashima, R. *Chem. Lett.* **1991**, 1491. (c) Mizutani, T.; Nakashima, R. *Chem. Lett.* **1991**, 2131.
(15) Whitten, J. L. *J. Chem. Phys.* **1963**, *39*, 349.

$$\langle \phi_{i0}\phi_{ia}|r_{ij}^{-1}|\phi_{j0}\phi_{jb}\rangle = \sum_m\sum_n\sum_p\sum_q c_m c_n c_p c_q \times \frac{2\pi^{5/2}}{(\alpha_m+\alpha_n)(\alpha_p+\alpha_q)(\alpha_m+\alpha_n+\alpha_p+\alpha_q)^{1/2}} \times \exp\left(-\frac{\alpha_m\alpha_n}{\alpha_m+\alpha_n}|\vec{R}_m-\vec{R}_n|^2-\frac{\alpha_p\alpha_q}{\alpha_p+\alpha_q}|\vec{R}_p-\vec{R}_q|^2\right) \times F_0\left(\frac{(\alpha_m+\alpha_n)(\alpha_p+\alpha_q)}{\alpha_m+\alpha_n+\alpha_p+\alpha_q} \times \left|\frac{\alpha_m\vec{R}_m+\alpha_n\vec{R}_n}{\alpha_m+\alpha_n}-\frac{\alpha_p\vec{R}_p+\alpha_q\vec{R}_q}{\alpha_p+\alpha_q}\right|^2\right)$$

$$\langle \phi_{i0}|\vec{r}_i|\phi_{ia}\rangle = \sum_m\sum_n c_m c_n\left(\frac{\pi}{\alpha_m+\alpha_n}\right)^{3/2} \times \exp\left(-\frac{\alpha_m\alpha_n}{\alpha_m+\alpha_n}|\vec{R}_m-\vec{R}_n|^2\right) \times \frac{\alpha_m\vec{R}_m+\alpha_n\vec{R}_n}{\alpha_m+\alpha_n}$$

$$\langle \phi_{jb}|\vec{r}_j\times\vec{\nabla}_j|\phi_{j0}\rangle = \frac{1}{2}\sum_p\sum_q c_p c_q\left(\frac{\pi}{\alpha_p+\alpha_q}\right)^{3/2} \times \exp\left(-\frac{\alpha_p\alpha_q}{\alpha_p+\alpha_q}|\vec{R}_p-\vec{R}_q|^2\right) \times \frac{\alpha_p\alpha_q}{\alpha_p+\alpha_q}\vec{R}_p\times\vec{R}_q$$

$$F_0(x) = \frac{1}{2}\left(\frac{\pi}{x}\right)^{1/2}\mathrm{erf}(\sqrt{x})$$

The matrix element and the electric transition moment involving ϕ_{jc} can be similarly obtained.[14a] For the Soret transition, CI calculations were carried out and the CI coefficients for the excited states α_1 and α_2 were used to calculate the electric transition moment and the matrix element as shown below.

$$\vec{\mu}_{i0a} = \alpha_1\langle\phi_{i0}|e\vec{r}|\phi_{ia1}\rangle + \alpha_2\langle\phi_{i0}|e\vec{r}|\phi_{ia2}\rangle$$

$$\langle \phi_{i0}\,\phi_{ia}|r_{ij}^{-1}|\phi_{j0}\,\phi_{jb}\rangle = \alpha_1\langle\phi_{i0}\,\phi_{ia1}|r_{ij}^{-1}|\phi_{j0}\,\phi_{jb}\rangle + \alpha_2\langle\phi_{i0}\,\phi_{ia2}|r_{ij}^{-1}|\phi_{j0}\,\phi_{jb}\rangle$$

The calculated electric transition moments (for the B_x and B_y bands) for **1** were parallel to the C5–C15 axis and the C10–C20 (the meso carbons) axis (Figure 4). This direction of the transition moment is in agreement with those reported for the iron porphyrin.[16] The magnetic transition moment of the carbonyl n–π^* transition and the electric transition moment of the carbonyl π–π^* transition were calculated based on the optimized geometry of glycine methyl ester and were almost parallel to the C=O axis. The magnetic transition moment was tilted by approximately 5° relative to the C=O axis, and the electric transition moment, by 13°. The glycine methyl ester was placed above the porphyrin plane with the carbonyl plane parallel to the porphyrin plane and the distance between the two planes was kept at 2.4 Å according to the geometry observed in a crystal of the Leu–OMe–**12** complex.[17] The angle θ was defined as shown in Figure 5. At $\theta = 45°$, the carbonyl carbon was above the pyrrole nitrogen. The carbonyl group was rotated by 15° increments and the rotational strength was calculated by the above equations for each configuration. The absorption maxima for the porphyrin Soret band and the carbonyl n–π^* and π–π^* bands were assumed to be 420, 210, and 170 nm, respectively. The former value is the experimentally observed value for host **1**, and the latter is that for ethyl acetate.[18]

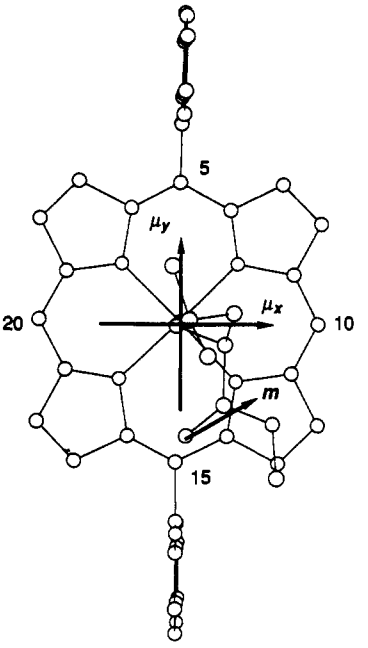

Figure 4. Electric (μ_x, μ_y) and magnetic (m) transition moments of Leu–OMe–host **1** complex. The electric transition moment of the carbonyl π–π^* transition is not shown but almost parallel to m.

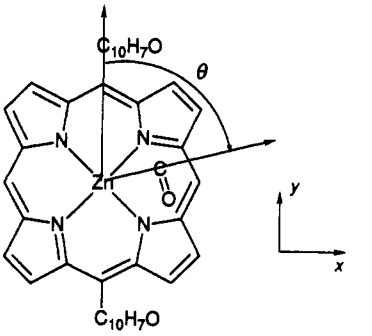

Figure 5. Coordinate and angle θ for the complex between host **1** and an amino acid ester used for molecular orbital calculations.

The results are shown in Figure 6. For a wide region of θ, the coupling between the magnetic transition moment (or the electric transition moment) of the carbonyl group and the electric transition moment of the porphyrin gives the rotational strength in an opposite sign in B_x and B_y. This is reasonable because the two electric transition moments B_x and B_y are perpendicular to each other, and if the magnetic transition moment (or the electric transition moment) bisects an angle between B_x and B_y, then the geometrical relationship between B_x and B_y is pseudoenantiomeric. The X-ray diffraction analysis of the crystals of a complex of Leu–OMe and **12** indicated that the C=O axis of the carbonyl group bisects an angle between the C5–C15 line and the C10–C20 line as shown in Figure 4.[17] In Figure 7, a possible geometry for the host **1**–L-Leu–OMe complex, which is deduced from the above X-ray diffraction results, is shown.[19] The angle θ is 135° for this conformation. The calculated values of R_a for this conformation are 5.7×10^{-40} and -3.4×10^{-40} cgs. These values are consistent with the experimental observation that the CD

(16) (a) Du, P.; Loew, G. H. *J. Phys. Chem.* **1991**, *95*, 6379. (b) Eaton, W. A.; Hofrichter, J. In *Methods in Enzymology*; Antonin, E., Rossi-Barnardi, L., Chiancone, E., Eds.; Academic Press: New York, 1981; Vol. 76, pp 175 .

(17) Ogoshi, H.; Masuda, H.; Uzawa, T.; Aoyama, Y. Unpublished results.

(18) (a) Schreibe, G.; Povenz, F.; Linström, C. F. *Z. Phys. Chem.* **1933**, *20*, 283. (b) Silverstein, R. M.; Bassler, G. C.; Morrill, T. C. *Spectroscopic Identification of Organic Compounds*; John Wiley & Sons, Inc.: New York, 1981.

(19) Geometry was optimized for all the atomic coordinates of the Leu–OMe and host **1** complex by use of the PM3 calculation.[12]

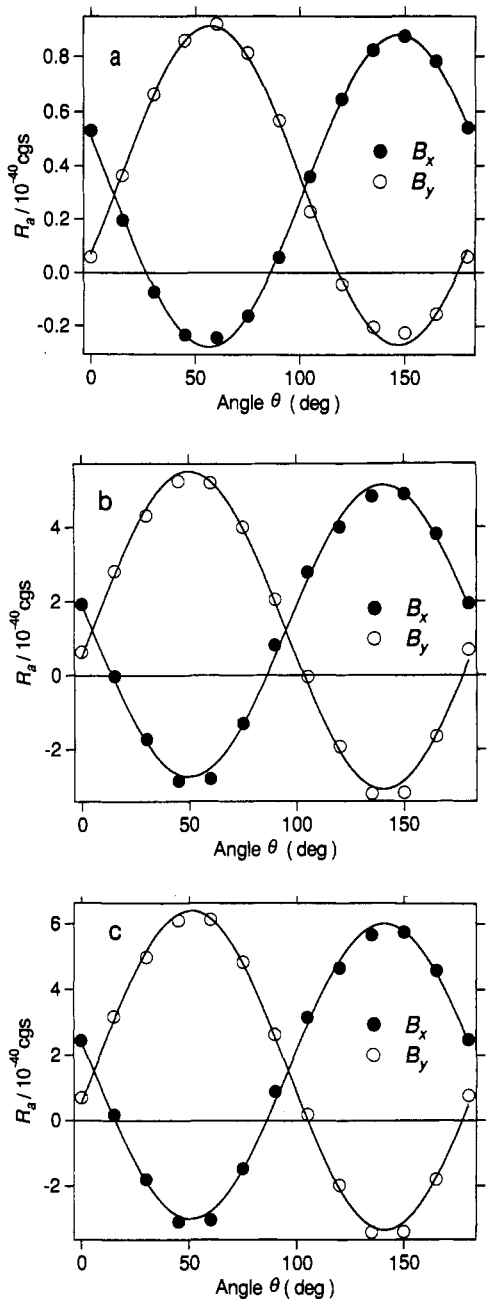

Figure 6. Rotational strength calculated by the perturbation approximation: (a) rotational strength arising from the coupling between the magnetic transition moment of the carbonyl group (n–π^* transition) and the electric transition moment of the porphyrin Soret transition (B_x and B_y); (b) rotational strength arising from the coupling between the electric transition moment of the carbonyl group (π–π^* transition) and the electric transition moment of the porphyrin Soret transition (B_x and B_y); (c) sum of the above two contributions.

spectrum exhibited split type ICD. The values of the rotational strengths obtained from the experiment were 32.3×10^{-40} and -36.5×10^{-40} cgs for the L-Leu–OMe–host **1** complex and 7.4×10^{-40} and -8.8×10^{-40} cgs for the L-Ala–OMe–host **1** complex.[20] The small calculated values are consistent with the results for unsaturated ketones, where the similar calculation gave the rotational strength one order of magnitude smaller than experiment.[21]

In order to explain the split type ICD based on the carbonyl–porphyrin coupling mechanism, we have to assume that the transition energy for the B_x transition and that for the B_y transition

(20) cgs = esu·cm·erg·G^{-1}

(21) Mizutani, T.; Ema, T.; Ogoshi, H. Unpublished results.

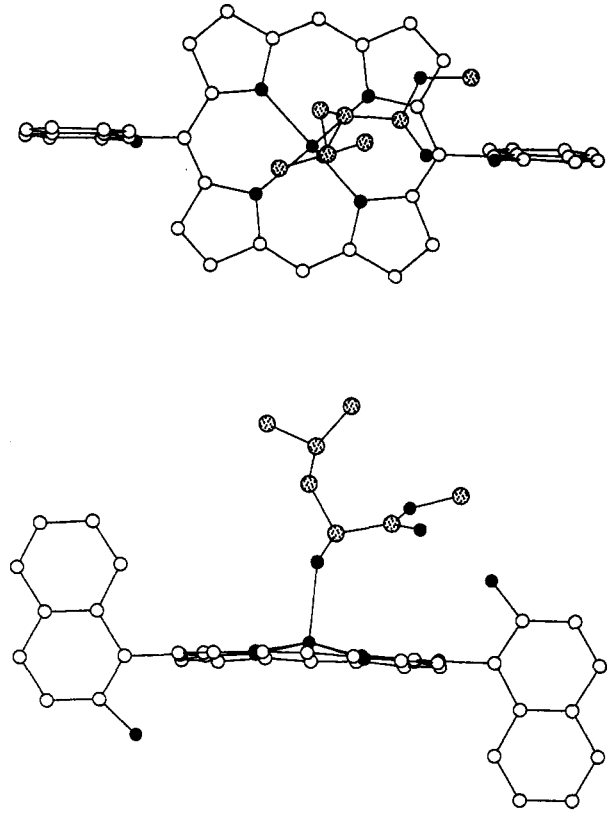

Figure 7. Possible geometry of the complex between L-Leu–OMe and host **1**. The geometry was optimized by PM3 molecular orbital calculations. In the calculations, ethyl groups on β-position of pyrrole were replaced by hydrogen. This conformer is similar to that observed for the Leu–OMe–Rh-porphyrin **12** complex in terms of the dihedral angle of N–C_α–C(carbonyl)–O. All hydrogen atoms are omitted for clarity.

should be different. Host **1** has two naphthyl groups at the meso position on the y axis and two hydrogens on the x axis. Therefore it is reasonable to assume that the transition energy of x polarization and that of y polarization will be different due to the substituent effects. This assumption is supported by the experimental observation that the difference in the values of λ_{max} between B_x and B_y is within 5–7 nm for all the host–guest complexes (Table 1). This also implies that the more symmetric porphyrins such as octaethylporphyrin do not tend to show split type ICD by this mechanism due to the degeneracy of the B_x and B_y transition. The triphenyl porphyrin **5**–L-Leu–OMe complex exhibited very weak ICD in the Soret region. The tetraphenyl porphyrin **11**–L-Leu–OMe complex exhibited almost no ICD in the Soret region. The half-width of the Soret band in the visible spectrum of **11** is 10 nm, narrower than that of **1** (14 nm), **3** (13 nm), and **5** (11 nm). This observation supports the above discussion that the three or four phenyl groups on the meso positions will cause near degeneracy of the B_x and B_y transition, thus reducing the intensity of the split ICD.

Most of the amino acid ester–host **1** complexes exhibited the ICD of positive and negative peaks in almost equal intensities. However the following three complexes showed the splitting ICD of positive and negative peaks in unequal intensities: (1) the complexes between aromatic amino acid ester–host **1**, (2) the complexes between Leu–OBu^t, Pro–OMe, and Glu–OMe and host **1**, and (3) the Leu–OMe–**3** complex (Table 1). The unsymmetrical ICD for aromatic amino acid esters can be explained by the additional contribution from the electric transition moment of the aromatic side chain. The unsymmetrical ICD observed for Leu–OBu^t, Pro–OMe, and Glu–OMe suggests that the carbonyl group is tilting in the hydrogen-bonding complex. In the correlation shown in Figure 3, a deviation of aromatic amino acids and leucinol can be reasonably explained by the

carbonyl–porphyrin coupling mechanism. The unsymmetrical splitting in the ICD observed for the Leu–OMe–3 complex may result from the slightly different configuration in the hydrogen-bonding complex. BOC–His–OMe did not exhibit any ICD in the Soret region. This may be ascribed to the completely different binding mode in the complex, where the nitrogen of the imidazole would coordinate to the zinc ion. With this interaction mode, the chiral carbon is far away from the porphyrin plane and the electric transition moment of the imidazole group becomes nearly perpendicular to the porphyrin plane. Only the components of the electric transition moment parallel to the porphyrin plane can make contributions to the ICD.[3] Therefore the ICD caused by BOC–His–OMe is expected to be small.

Porphyrin Plane Puckering Mechanism. Some porphyrins such as peripherally crowded ones[22] and nickel complexes of porphyrins[23] were reported to be nonplanar. Steric hindrance and coordination to a small metal ion are suggested to be the driving forces of nonplanarity, respectively. Therefore it is possible that the induced CD observed in the present system is also caused by the complexation-induced puckering of the porphyrin plane. In a typical puckered porphyrin, (2,3,7,8,12,13,17,18-octaethyl-5,-10,15,20-tetraphenylporphyrinato)zinc(II), a red shift of 50 nm in the Q-band and one of 35 nm in the Soret band were observed, and this is considered as good evidence for the puckering along with the other experimental and theoretical results.[22,23] In the present system, absorption maxima of host **1** are normal, indicating that no puckering occurred in an uncomplexed state. The Soret peak maximum of the complex between L-Leu–OMe and the methoxy derivative **2**, where no hydrogen bonding was observed and almost no ICD was observed, was the same as that of the L-Leu–OMe–host **1** complex (428 nm). In the case of amino acid ester–host **1** complexes, the peak separation between the B_x peak and the B_y peak ranged from 5 to 7 nm, and can be considered as constant as the structure of amino acid esters changed. These observations rather support the carbonyl–porphyrin coupling mechanism because the carbonyl–porphyrin coupling mechanism implies that the difference in the transition energies for the perpendicularly polarized transition is determined by the naphthyl substituent and should not vary with varying the guest structure. In contrast to that, according to the puckering mechanism the difference in the transition energies for the perpendicularly polarized transition can be varied depending on the extent of puckering caused by the intermolecular interactions. Therefore the peak separation and the rotational strength can be correlated contrary to the experimental observations. Molecular orbital calculations by the PM3 method also predict that the porphyrin plane in the Leu–OMe–host **1** complex is almost planar (Figure 7), while the calculation by the same method is able to predict the nonplanarity of (2,3,7,8,12,13,17,18-octaethyl-5,10,15,20-tetraphenylporphyrinato)zinc(II).[24] However we have little information on the relationship between the degree of puckering and the intensity of the induced CD. Other good models will be required to investigate this interesting problem.

Implications to the Origin of the Induced CD of Hemoproteins. The CD induced in the Soret region of hemoprotein has been utilized as an useful probe of conformational changes of proteins. The induced CD of myoglobin is primarily ascribed to the coupling with surrounding aromatic side chains of His, Phe, and Tyr.[3] Contribution from the peptide backbone is considered to be minor. The rotational strength in human oxy-, deoxy-, and methemoglobin was determined to be 21, 35, and 28 × 10^{-40} cgs, respectively.[3] These values are comparable to those observed in our system (Table 1). The fact that only one chiral center can induce the same magnitude of ICD as those of hemoprotein indicates that the ICD of hemoprotein is caused by cancellation of many elemental interactions.[3] In the present two-point fixation systems (hosts **1** and **3**), a comparison of the rotational strength between aromatic amino acid esters (R_a of (19–51) × 10^{-40} cgs) and aliphatic ones (R_a of (18–37) × 10^{-40} cgs) indicates that the additional contribution from the coupling to aromatic side chain is appreciable but not dominant (Table 1). In the one-point fixation system (hosts **2**, **6**, and **7**), the ICD was also observed for the complex between aromatic amino acid esters and host **2**, where the guest molecule can be rotating around the (host)Zn–N(guest) bond. This demonstrates that the aromatic side chain makes a contribution to the ICD even if it is not fixed. This is in sharp contrast with the carbonyl chromophore, which makes almost no contribution to the ICD when freely rotating. Thus, the complexes between aliphatic amino acid esters and host **2** did not exhibit any ICD, where the amino acid esters are freely rotating. The results shown in Table 1 indicate that coupling with aliphatic side chains (Me, Pr^i, Bu^i, $CH_2CH_2COOCH_3$, CH_2COOCH_3) is negligibly small. In hemoprotein, the aromatic side chains may be relatively fixed owing to the three-dimensional structure of the proteins. The aromatic group in our model system may be rotating, and the ICD caused by the aromatic side chain was reduced. It is noteworthy that the coupling with the carbonyl group is more important than the coupling with aromatic side chains for the present system. However, the present results do not necessarily mean that the peptide carbonyl group should be more important for the ICD in the case of hemoproteins[25] because the mobility of the side chains in the present host–guest complexes is not particularly controlled. A three- or four-points recognition host should be designed and synthesized to investigate the contribution of the side chain chromophores to the ICD.

Acknowledgment. We are grateful for the kind help by Dr. M. Hada for molecular orbital calculations. Numerical calculations were carried out either on a Hewlett-Packered Apollo 9000 workstation, a Silicon Graphics IRIS Indigo XS 24 workstation or a FACOM VP-2600 at the Data Processing Center of Kyoto University. This work was supported by a Grant-in-Aid for Specially Promoted Research (No. 04101003) from the Ministry of Education, Science, and Culture, Japan.

(22) (a) Thompson, M. A.; Zerner, M. C. *J. Am. Chem. Soc.* **1988**, *110*, 606. (b) Barkigia, K. M.; Chantranupong, L.; Smith, K. M.; Fajer, J. *J. Am. Chem. Soc.* **1988**, *110*, 7566. (c) Barkigia, K. M.; Berber, M. D.; Fajer, J.; Medforth, C. J.; Renner, M. W.; Smith, K. M. *J. Am. Chem. Soc.* **1990**, *112*, 8851.

(23) Shelnutt, J. A.; Medforth, C. J.; Berber, M. D.; Barkigia, K. M.; Smith, K. M. *J. Am. Chem. Soc.* **1991**, *113*, 4077.

(24) X-ray crystallographic analysis of zinc octaethyltetraphenylporphyrin showed that β protons of pyrrole rings were displaced by *ca.* 1 Å relative to the plane of the four nitrogen atoms.[22b] The calculation by the PM3 method showed that the displacement was approximately 0.45 Å.

(25) The rotational strength arising from the coupling between the porphyrin Soret transition and the benzene π–π^* transition was calculated by use of the same program in order to compare the relative importance of the carbonyl and aromatic chromophores. The benzene ring was placed with its plane parallel to the porphyrin plane and the distance between the two planes was 2.4 Å. The coupling between the electric transition moment of the benzene transition and the Soret electric transition moments B_x and B_y was thus calculated. The angle between the benzene transition moment and the y axis in Figure 5 was $\theta = 135°$. The rotational strength was 11.7 × 10^{-40} esu-cm-erg-G^{-1} for the B_x transition and −13.8 × 10^{-40} esu-cm-erg-G^{-1} for the B_y transition, respectively. These values were 2–4 times larger than those arising from the coupling with the carbonyl π–π^* transition. This result implies that the aromatic chromophore makes more important contributions to the ICD when fixed than the carbonyl chromophore.